ISSN 1027-5495. Functional Materials, 23, No.2 (2016), p. 268-273.
doi:http://dx.doi.org/10.15407/fm23.02.268

A semiempirical description of functionalized nanodiamonds with NV^- color centers

***A.V.Luzanov*[1], *O.A.Zhikol*[1], *I.V.Omelchenko*[1], *A.P.Nizovtsev*[2], *S.Ya.Kilin*[2], *A.L.Puchkarchuk*[3], *V.A.Puchkarchuk*[4]**

[1] SSI "Institute of Single Crystals", National Academy of Sciences of Ukraine, 60 Nauky Ave., 61078 Kharkiv, Ukraine
[2]B.Stepanov Institute of Physics, National Academy of Sciences of Belarus, 68 Prosp. Nezavisimosti, 220072 Minsk, Belarus
[3]Institute of Physical Organic Chemistry, National Academy of Sciences of Belarus, 13 Surganova Str., 220072 Minsk, Belarus
[4]Belarusian State University of Informatics and Radioelectronics, 6 P.Brovki Str., 220013 Minsk, Belarus

Received December 21, 2015

Possibilities of semiempirical AM1 method in descripting the nanodiamond spectral properties are investigated with the stress on the relevant functionalized systems containing nitrogen-vacancy color centers. We studied two types of functionalization — hydroxylation and fluorination of the nanodiamond surface. It is shown that only slight spectral shifts occur (batochromic shifts in case of the hydroxylation, and hypsochromic ones in case of the fluorination). The semiempirical approach demonstrates the ability to easily and simply handle nanoclusters with hundreds carbon atoms.
Keywords: nitrogen-vacancy center, AM1 method, spectral shifts, HOMO-LUMO gap.

Исследованы возможности полуэмирического метода AM1 для вычислений спектральных свойств наноалмазов с акцентом на подходящие функционализированные системы, содержащие азот-вакансионные центры окраски. Изучено два типа функционализации поверхности наноалмазов — гидроксилирование поверхности и ее фторирование. Показано, что имеют место только слабые спектральные сдвиги — батохромные при гидроксилировании и гипсохромные при фторировании поверхности. Полуэмпирический подход демонстрирует способность легко исследовать нанокластеры с сотнями углеродных атомов.

Напівемпіричне описування функціоналізованих наноалмазів з NV^--центрами забарвлення. *А.В.Лузанов, О.А.Жикол, І.В.Омельченко. А.П.Нізовцев, С.Я.Кілін, А.Л.Пушкарчук, В.Я.Пушкарчук.*

Досліджено можливості напівемпіричного методу AM1 щодо розрахунку спектральних властивостей наноалмазів з акцентом на відповідні функціоналізовані системи, що містять нітроген-вакансійні центри забарвлення. Вивчено два типи функціоналізації — гідроксилювання та флуорування поверхні наноалмазів. Виявлено, що відбуваються тільки слабкі спектральні зсуви — батохромні за гідроксилювання поверхні та гіпсохромні за її флуорування. Напівемпіричний підхід демонструє здатність легко трактувати нанокластери із сотнями вуглецевих атомів.

1. Introduction

In many respects, nanodiamonds are very attractive materials which can be employed in a wide range of applications [1–4]. One of the potential applications of nanodiamonds is their usage in advanced quantum informa-

tion processing [3]. In this field, the photostable diamond nitrogen-vacancy color center (NV^- center) is considered as a promising candidate for a quantum bit (qubit). This and other challengs will likely require a variety of modified and functionalized nanodiamonds [5–8]. A lot of theoretical works deals with functionalization of nanodiamond surface, but only few are related to the functionalized diamondoids with NV^- defects [9–12]. The aim of this contribution is to explore the ability of some typical semiempirical models for predicting spectral effects of surface functionalization in nanodiamonds with the color centers.

2. Crude estimations by perturbative one-electron method

We first use a very simple model traditionally named the extended Huckel theory (EHT). It is based on the tight-binding approximation for all valence electrons (see the pivotal paper [13] and further developments in [14–17]). In this approach one deals with one-electron molecular orbitals (MOs) constructed from valence atomic orbitals (AOs). The latter are characterized by effective ionization potentials (IPs), and for the atoms of the second period elements, these are $2s$ and $2p$ ionization energies W_{2s} and W_{2p}. Furthermore, the Slater AO overlap integrals are additionally invoked when computing the effective EHT Hamiltonian matrix. Solving a generalized eigenvalue problem for this matrix routinely produces a set of orbital energies, ε_j, and corresponding MOs φ_j. Most important are the so-called frontier orbitals, HOMO (highest occupied) and LUMO (lowest unoccupied) molecular one-electron energy levels. They determine the lowest excitation energy, chemical reactivity, and plenty of other properties.

In the case of open-shell molecular states, not all the electrons are paired in the occupied MOs, and moreover MOs can be different for spin-up and spin-down electrons. However, there is no difference between the spin-up and spin-down EHT orbitals; only occupation numbers for these MOs vary in dependence of the total spin of the state in study. For instance, consider the triplet state of a $2n$-electron system (n is an integer). In the conventional one-electron description, the singlet ground state is constructed by pairwise filling the first (lowest in the energy ε_j) n single-particle levels as follows: $|\varphi_1\ \overline{\varphi}_1\ \ldots\ \varphi_n\ \overline{\varphi}_n\ \rangle$. Here a bar above φ_j signifies the spin-down state of the corresponding electron, and the lack of the bar indicates that φ_j is the spin-up state. In this notation, the lowest EHT triplet state gets the form:

$$|\varphi_1\overline{\varphi}_1\ldots\varphi_{n-1}\overline{\varphi}_{n-1}\varphi_n\varphi_{n+1}\rangle. \qquad (1)$$

In particular, orbital construction (1) provides a good model of the ground triplet state in the non-symmerical nanodiamonds with negatively charged NV^- centers. As a possible excited triplet state, we consider $|\varphi_1\ \overline{\varphi}_1\ \ldots\ \varphi_{n-1}\ \varphi_n\ \overline{\varphi}_n\ \varphi_{n+1}\rangle$ which corresponds to one-electron transition $\overline{\varphi}_{n-1} \to \overline{\varphi}_n$.

The associated transition energy is

$$\lambda = \varepsilon_n - \varepsilon_{n-1}. \qquad (2)$$

This type of excitation occurs in particular in nanodiamonds with the defects which we study in the paper. Evidently, ε_n is the energy of HOMO φ_n, and ε_{n-1} is energy of the second-highest occupied MO φ_{n-1}, named usually HOMO-1. Notice that adopting this notation we implicitly consider all MOs in respect to the "ground" singlet state even in the case when this state lies above the lowest triplet state (as in our objects, NV^--centers).

Now we can discuss how to approximately estimate the electron effects produced by local change in the atomic structure of surface. We assume that in terms of the EHT Hamiltonian the above change makes IP of the modified surface atom other than that in the initial (unperturbed) system. With this, we imply that the IP alteration is quite small, so we can apply a counterpart of the Coulson-Longuet-Higgins perturbation method (MO reactivity indices [18–20]). More specifically, let W_A be the IP of an atom A in the studied system, and let the atom A be perturbed so that $W_A + \delta W_A$ is the new IP of the atom, where the added magnitude δW_A is suggested to be relatively small. Then the appropriate difference in any electronic quantity Z is approximately given by $\delta Z = \delta W_A(\partial Z/\partial W_A)_0$ where the derivative $\partial Z/\partial W_A$ is computed either analytically by the ordinary perturbation method, or simply by numerical differentiation. In particular, the expression

$$\delta\lambda = \delta W_A(\partial\lambda/\partial W_A)_0 \qquad (3)$$

can be used for a crude estimate of the spectral shift $\delta\lambda$ in the perturbed system.

After this preliminary, we can apply the above MO perturbation approach, which is more or less familiar, to the NV^--containing nanodiamond cluster previously treated in [21]. Specifically, we take the finite-size structure of composition $C_{98}H_{72}N^-$ (see the image in Table 3 in loc. cit.) and make a small perturbation δW_{2p} in W_{2p} for a successive set of the carbon atoms. We start from the nearest neighbor of the nitrogen atom (inside the cluster) and move towards surface atoms. The results for the lowest energy excitation λ, Eq. (2), and orbital localizations are given in Table 1. We see that all the quantities, while oscillating, rapidly decline with the distance between the nitrogen and perturbed carbon atoms. Thus, the surface modification will make only little influence upon excitation energy (2) as well as on other electronic properties of NV^- centers. The result is in concordance with the fact that the low-lying electron transition (i.e., HOMO-1 $\rightarrow$ HOMO at the EHT level) is strongly localized in a vicinity of the NV^- center as clearly demonstrated in [22]. Thus, based on the simple one-electron all-valence scheme we can expect insignificant electronic effects of the surface functionalization of nanodiamonds with NV^- defects.

Table 1. Distance dependence of excitation energy derivative $(\partial\lambda/\partial W_A)_0$, and unperturbed HOMO and HOMO-1 localizations (the squared expansion coefficients) on the perturbed carbon atoms. In abscissa, R is the distance (in Å) between the nitrogen atom and the corresponding perturbed atom of cluster $C_{98}H_{72}N^-$

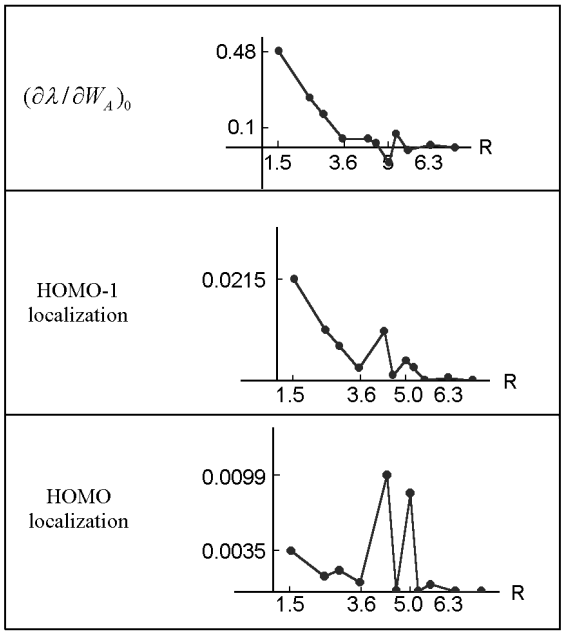

3. Semiempirical estimations by AM1 method

The above crude analysis can be refined by supplementing it with a more consistent semiempirical approach. More precisely, we employed the standard AM1 semiempirical method to obtain the electronic spectra of the three NV^--containing nanodiamond structures ($C_{98}H_{72}N^-$, $C_{188}H_{110}N^-$, and $C_{428}H_{212}N^-$) and their surface-functionalized species. Note that all the constructed clusters have idealized geometry built as a part of the bulk diamond structure (d(C–C) = 1.54 Å) by removing a carbon atom and changing a neighbor of the atom to nitrogen atom. The configuration interaction singles (CIS) calculations at the UHF (unrestricted Hartree-Fock) level for AM1 hamiltonian was performed with the G09 package [23]. The functionalization of the clusters was made in two ways: 1) surface hydroxylation (replacing all CH groups by COH groups); and 2) surface fluorination (replacing all CH groups by CF groups). The results are given in Table 2. In this Table we present also spin densities for the triplet ground state of the NV^- color centers. As in studies [24–26] and in our previous work [21], the predominant contribution to the overall spin distribution is made by the three valence-unsaturated atoms in vicinity of the vacancy (referred to as atoms C_α, C_β and C_γ in Table 2). Notice that for the finite-size clusters considered here, the quasidegenerate excited state energies ($\lambda_1 \cong \lambda_2$) agree with the empirical estimation [27] $\lambda \cong$ 2.2 eV at least semiquantitatively. Despite using unrestricted open-shell MOs, a spin purity of all the states considered is quite good. A typical average value of the squared spin operator $<S^2>$ is 2.02 for the ground state, and 2.04 for the excited states. It clearly ascribes a triplet nature to the states. As to the functionalization effect proper, we can state that indeed even the significant perturbation of the cluster surface (e.g., the hydroxylation of all CH groups) can produce only small spectral effects. It is in concordance with the qualitative estimations of the previous section. This important feature of surface functionalization allows to design new materials with better solubility and other useful properties without damaging valuable optical characteristics of color centers inside the nanodiamond bulk. From Table 2 we can

Table 2. The energy gap Δε, the lowest triplet-triplet excitation energies λ_1 and λ_2 (all in eV), oscillator strengths (in parentheses), and the ground-state spin-density distribution near the close vicinity of color center

Cluster		Δε	λ_1	λ_2	Spin density on C_α, C_β, C_γ
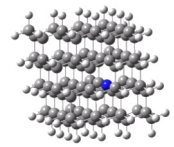	$C_{98}H_{72}N^-$	7.27	1.716 (0.071)	1.852 (0.060)	0.682, 0.720, 0.664
	$C_{98}H_{60}NO_6^-$	7.22	1.699 (0.074)	1.871 (0.060)	0.672, 0.729, 0.665
	$C_{98}H_{12}F_{60}N^-$	7.40	1.720 (0.070)	1.913 (0.54)	0.685, 0.742, 0.660
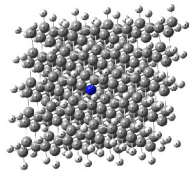	$C_{188}H_{110}N^-$	7.25	1.748 (0.057)	1.749 (0.057)	0.686, 0.686, 0.686
	$C_{188}H_{110}NO_{98}^-$	6.78	1.725 (0.063)	1.771 (0.063)	0.698, 0.687, 0.676
	$C_{188}H_{12}F_{98}N^-$	7.40	1.755 (0.056)	1.755 (0.056)	0.688, 0.688, 0.688
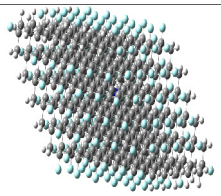	$C_{428}H_{212}N^-$	6.97	1.719 (0.074)	1.761 (0.059)	0.683, 0.696, 0.680
	$C_{428}H_{212}NO_{152}^-$	5.89	1.693 (0.082)	1.779 (0.059)	0.671, 0.706, 0.683
	$C_{428}H_{60}F_{152}N^-$	7.25	1.723 (0.057)	1.764 (0.074)	0.694, 0.689, 0.677

also see that enlarging cluster size slightly affect electronic transitions.

In this connection a few words should be said about symmetry of the lowest triplet states of the NV^- center. In the regular diamond and nanodiamondoid lattices, NV^- point defects possess C_{3v} symmetry [2]. The ground state of these defects has $^3A_2$ symmetry whereas the first excited state is the two-fold degenerate ^3E state. In low-symmetry structures, this ^3E term is split, which is the case of the systems studied here. Turning back to Table 2 we see that for the first transition, the hydroxylation produces a batochromic effect, becoming smaller with increasing cluster size. The second transition, on the contrary, undergoes a hypsochromic shift. In average, the two quasidegenerate transitions undergo a small batochromic shift (e. g., 0.003 eV for $C_{428}H_{212}N^-$). Analogously, the fluorination gives rise to a marked hypsochromic effect (0.004 eV for $C_{428}H_{212}N^-$). For the ground state of the NV^- centers, we observe a small redistribution in atomic spin densities in the closest to the vacancy carbon atoms; the overall spin density in this region remains stable (close to 2.06).

The conventional orbital gap

$$\Delta\varepsilon = \varepsilon_{LUMO} - \varepsilon_{HOMO} \qquad (4)$$

Table 3. Description of the $C_{98}H_{72}O_nN^-$ cluster face, the two lowest triplet-triplet excitation energies λ (in eV), oscillator strengths f (in parentheses), and averaged excitation energy λ_{mean} (in eV) for anisotropic functionalization

i	$d(N)$	α	λ (f)	λ_{mean}
6	5.5	19.5	1.712 (0.071)	1.786
			1.859 (0.062)	
6	6.1	−19.5	1.703 (0.076)	1.786
			1.869 (0.059)	
8	5.5	19.5	1.699 (0.072)	1.785
			1.871 (0.061)	
8	6.1	−19.5	1.745 (0.071)	1.794
			1.843 (0.067)	
8	3.5	19.5	1.675 (0.077)	1.789
			1.903 (0.058)	
8	4.0	−19.5	1.684 (0.074)	1.788
			1.892 (0.061)	
8	4.0	90	1.704 (0.071)	1.787
			1.870 (0.061)	
8	5.5	−90	1.667 (0.074)	1.788
			1.908 (0.058)	

which is also displayed in Table 2, provides an additional useful information. Taking into account Eqs. (1) and (2) which are valid for the restricted open-shell Hartree-Fock (ROHF) theory, we understand that within UHF we must use in Eq. (4) the spin-down HOMO and LUMO orbital energies. At the same time, in framework of CIS and any configuration-interaction approach, this gap is no longer the lowest excitation energy (as is wrongly thought sometimes, see discussion in [28]). However, $\Delta\varepsilon$ can be roughly identified [29] with the chemical hardness $I-A$ (I is the ionization potential, and A the electron affinity of the state considered). Looking at Table 2, we see that the HOMO-LUMO gap values are symbatic with excitation energies. Then, in Pearson's terms of hardness and softness, this means that the fluorination increases the electronic hardness of the clusters whereas the hydroxylation increases their electronic softness.

The usual chemical functionalization of the nanodiamond surface is expected to be more or less isotropic. It means an approximately equal number of functional groups over each nanoparticle face, with small enough surface density of the groups. A limiting anisotropic case, where a single face is fully functionalized and others contain no functional groups, should be considered as a model probably remaining within the reach of the contemporary synthetic techniques. On the other hand, the case is theoretically important due to an appreciable perturbation created by the functionalized face in the vicinity of NV^- color center.

We study the case on the example of our smallest cluster, $C_{98}H_{72}N^-$. The exhaustive face functionalization means for the cluster either 6 (on 2 faces) or 8 (on 6 faces) hydroxogroups. For characterizing the defect position in respect to a face, two parameters are required. The first one is the distance from the nitrogen atom to the mean-square plane of the oxygen atoms, $d(N)$. The second one is the angle α between the face and the directed line nitrogen $\rightarrow$ vacancy, calculated as 90° minus angle value between the line and the plane normal. The "+" sign for the angle is choosen arbitrary when the line exits from the face plane (vacancy is farther from the plane than the nitrogen atom), the "−" sign is choosen otherwise.

Table 3 contains the two lower excitation energies for 8 different one-face functionalized clusters $C_{98}H_{72}O_jN^-$. The average excitation energy for the two lowest quasidegenerated states remains the same within 0.01 eV. Thus, the functionalization anisotropie does not have any systematical and directed influence on the color center. The splitting of the levels due to the symmetry breaking may, however, be considerable enough (within 0.25 eV). It is expectedly larger when the NV^- center is closer to the modified surface, see the line of the table with $d(N)$ = 3.5 Å. The two last rows of the table show clearly that the splitting is also substantially larger when the vacancy is closer to the modified surface (due to the interatomic distance 1.54 Å, the whole color center is in these structures at the same distance from the modified surface). However all these details lose their significance with the cluster size increase, where the local NV^--center symmetry is barely distorted by the surface modifications on the cluster periphery.

4. Conclusion

In the present paper we studied the functionalized nanodiamond models by semiempirical methods. We found that the conventional AM1 computations provide reasonably satisfactory results for nanodiamonds with NV^- color centers. It gives us a hope to obtain semiqualitative results for huge nanodiamond structures which at present cannot be handled with facility by more advanced quantum chemistry methods. The semiempirical PM3 method (which is closely related to AM1) may be also useful here, as the results of several calculations (not reported here) confirm this. At the same time, other popular semiempirical techniques, such as ZINDO/S, are unable to provide even qualitatively a meaningful description of the low-lying electronic transitions in large NV^--containing structures. Thus, a certain caution should be taken in applying even AM1 and PM3 for large-scale systems and for non-idealized nanodiamond geometry. More work is needed to understand possible pitfalls that can catch the researcher in this field. As usual, sample testing by reliable *ab initio* methods is mandatory for the problems of this type.

Acknowledgment. This work was supported by the joint project of the National Academy of Sciences of Ukraine and the National Academy of Sciences of Belarus (Grant No. 09-06-15).

References

1. CVD Diamond for Electronic Devices and Sensors, ed. by R.S.Sussmann, Wiley, Berlin (2009).
2. Optical Engineering of Diamond, ed. by C.R.P.Mildren, J.R.Rabeau. Wiley, Berlin (2013).
3. Quantum Information Processing with Diamond, ed. by S.Prawer, I.Aharonovich, Elsevier, Cambridge (2014).
4. R.Schirhagl, K.Chang, M.Loretz et al., *Annu. Rev. Phys. Chem.*, **65**, 83 (2014).
5. Y.Xing, L.Dai, *Nanomedicine*, **4**, 207 (2009).
6. I.P.Chang, K.C.Hwang, J.-a.A.Ho et al., *Langmuir*, **26**, 3685 (2010).
7. K.-M.C.Fu, C.Santori, P.E.Barclay et al., *Appl. Phys. Lett.*, **96**, 121907 (2010).
8. M.V.Hauf, B.Grotz, B.Naydenov, *Phys. Rev. B*, **83**, 081304 (2011).
9. I.Kratochvilova, A.Kovalenko, A.Taylor et al., *Phys. Stat. Sol. (a)*, **207**, 2045 (2010).
10. H.Pinto, R.Jones, D.W.Palmer et al., *Phys. Rev. B*, **86**, 045313 (2012).
11. H.Pinto, D.W.Palmer, R.Jones et al., *J. Nanosci. Nanotechnol.*, **12**, 8589 (2012).
12. M.Kaviani, P.Deak, B.Aradi et al., *Nano Lett.*, **14**, 4772 (2014).
13. R.Hoffmann, *J. Chem. Phys.*, **39**, 1397 (1963).
14. G.Blyholder, C.A.Coulson, *Theoret. Chem. Data*, **10**, 316 (1968).
15. L.Lohr, P.Pyykko, *Chem. Phys. Lett.*, **62**, 333 (1979).
16. J.Cerda, F.Soria, *Phys. Rev. B*, **61**, 7965 (2000).
17. A.V.Akimov, O.V.Prezhdo, *J. Math. Chem.*, **53**, 528 (2015).
18. C.A.Coulson, H.C.Longuet-Higgins, *Proc. Roy. Soc. A*, **191**, **39 (1947); ibid, 192**, 16 (1947).
19. A.Streitwieser, Molecular Orbital Theory for Organic Chemists, Wiley, New York (1961).
20. M.Gonzalez-Suarez, A. Aizman, R.Contreras, *Theor. Chem. Acc.*, **126**, 45 (2010).
21. A.V.Luzanov, *Functional Materials*, **22**, 514 (2015).
22. A.V.Luzanov, O.A.Zhikol, *Functional Materials*, **23**, 63 (2016).
23. M.J.Frisch, G.W.Trucks, J.B.Schlegel et al., Gaussian 09, Revision C.01; Gaussian, Inc.: Wallingford, CT, USA (2010).
24. V.A.Pushkarchuk, S.Ya.Kilin, A.P.Nizovtsev et al., *Optics and Spectroscopy*, **99**, 245 (2005); ibid, **108**, 247 (2010).
25. A.S.Zyubin, A.M.Mebel, M.Hayash, *J. Comput. Chem.*, **30**, 119 (2009).
26. A.Ranjbar, M.Babamoradi, M.H.Saani et al., *Phys. Rev. B*, **84**, 165212 (2011).
27. Y.Ma, M.Rohlfing, A. Gali, *Phys. Rev. B*, **81**, 041204 (2010).
28. S.Larsson, Chemical Physics: Electrons and Excitations, Taylor & Francis, Boca Raton (2012).
29. G.G.Pearson, Chemical Hardness: Applications from Molecules to Solids, Wiley-VCH, Weinheim (1997); W.O.Yang, R.G.Parr, *Proc. Nat. Acad. Sci.*, **82**, 6723 (1985).